nature energy

SUPPLEMENTARY INFORMATION
https://doi.org/10.1038/s41560-018-0159-3

In the format provided by the authors and unedited.

Impact of myopic decision-making and disruptive events in power systems planning

Clara F. Heuberger[1,2], Iain Staffell[1], Nilay Shah[2,3] and Niall Mac Dowell[1,2]*

[1]Centre for Environmental Policy, Imperial College London, London, UK. [2]Centre for Process Systems Engineering, Imperial College London, London, UK. [3]Department of Chemical Engineering, Imperial College London, London, UK. *e-mail: niall@imperial.ac.uk

Supplementary Information for article 'Impact of myopic decision making and disruptive events in power systems planning' by Clara F. Heuberger, Iain Staffell, Nilay Shah, and Niall Mac Dowell

Contents

Supplementary Figure 1: The ESO model framework

Supplementary Figure 2: Scenario visualisation

Supplementary Figure 3: Cost reduction of SMR technology

Supplementary Table 1: Build rate parameter for technology type in GW/year for scenario 1,2, and 3

Supplementary Table 2: Data Sources

Supplementary Note 1: Acronyms

Supplementary Note 2: Model Assumptions

Supplementary Note 3: Mathematical Model Formulation
- Nomenclature
- System design constraints
- Unit commitment variables
- System wide power balance, security, and emission constraint
- Technology specific unit commitment, power and ancillary service constraints
- Unit up-time and down-time constraints
- Storage operation constraints
- Endogenous cost reduction
- Objective function

Supplementary Note 4: Parameterisation of the "unicorn technology"

Supplementary Note 5: Cost reduction of CLC-CCS associated to CO_2 transport and storage network

Supplementary Note 6: Solution Strategies
- Hourly Data Processing and Relaxation

Supplementary Note 7: Myopic Foresight
- Review of existing work
- Rolling horizon optimisation

Supplementary Discussion
- Scenarios with Small Modular Nuclear Reactors and increased availability battery storage as "super technology"
- Additional sensitivity analysis
  - Electricity demand
  - Fuel price

Supplementary References

Supplementary Figure 1

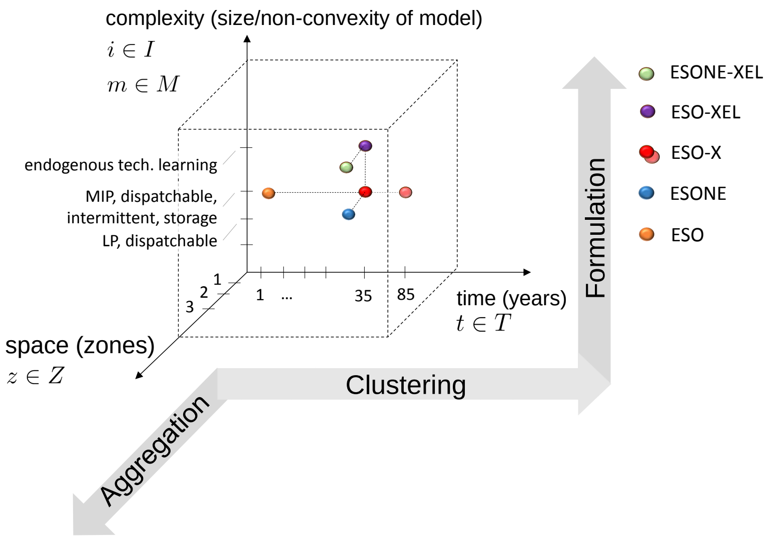

Supplementary Figure 1: Facets of the ESO modelling framework.

Supplementary Figure 2

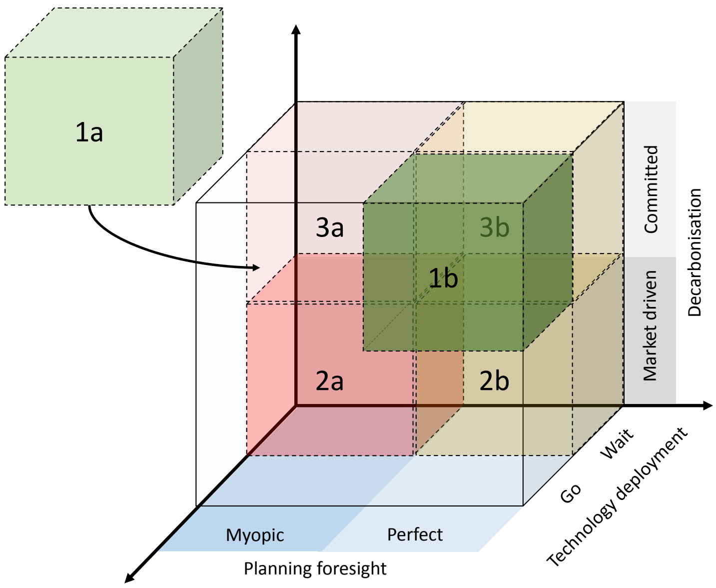

Supplementary Figure 2: Scenario visualisation.

Supplementary Figure 3

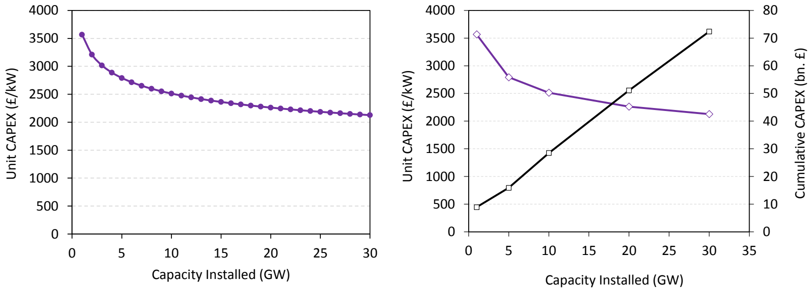

Supplementary Figure 3: Unit cost reduction assumptions for Small Modular Reactor (SMR) capacity deployment (left), as piecewise linear function (right, diamonds), as piecewise cumulative cost curve (right, squares). The capital cost of Small Modular Reactors (SMRs) are modelled in two ways in this work: first, at constant capital cost according to supplementary table 3, second, following a cost reduction curve based on the technology learning curve theory as presented in section supplementary note 5 and represented in equation 41. Following expert estimations by Abdulla and Roulstone [1, 2], we choose a learning rate of 10 % for SMR units. The piecewise linear cumulative cost curve is modelled in the ESO framework according to constraints 35 - 39, see section supplementary note 3.

Supplementary Table 1

Scenario	1	2	3
Nuclear	0.96	0.48	0.96
Coal	0	0	0
IGCC	0.25	0.25	0.25
CCGT	0.9	1.05	0.9
OCGT	0.5	0.5	0.5
Coal-CCS	0.25	0	0
CCGT-CCS	0.375	0	0
BECCS	0.25	0	0
Onshore-Wind	1.6	1.7	1.7
Offshore-Wind	1.5	1.75	1.75
Solar PV	1.5	1.5	1.5
HVDC (FR)	1	1	1
HVDC (IE, NL)	1	1	1
Pumped hydro	0.6	0.6	0.6
Lead-acid battery	0.5	0	0
Super technology	0	1	0

Supplementary Table 1: Build rate parameter for technology type in GW/year for scenario 1,2, and 3. Note that the build rate of the super technology is adjusted to either 0 or 1 in scenario 1 and 3 for the results presented in figure 4 of the main paper.

Supplementary Table 2

Input data category	Data sources reviewed
Power generation and storage technologies	
Nuclear	[3, 4, 5, 6, 7, 8]
Coal (super-critical)	[9, 10, 11, 12, 13, 14, 15, 16, 17, 6, 18, 8]
Integrated gasification combined cycle (IGCC)	[9, 10, 11, 13, 14, 10, 16, 17, 6, 19, 8]
Combined cycle gas turbine (CCGT)	[9, 20, 10, 21, 22, 14, 12, 23, 15, 16, 17, 7, 18, 8]
Open cycle gas turbine (OCGT)	[21, 22, 14, 12, 24, 15, 5, 17, 7, 18, 8]
Coal post-combustion CCS	[25, 9, 26, 11, 14, 13, 16, 19, 6, 7, 18, 8]
CCGT post-combustion CCS	[9, 20, 26, 11, 14, 23, 16, 10, 19, 7, 18, 8]
Bioenergy with CCS (BECCS)	[13, 19, 27, 28, 29]
Onshore Wind	[30, 21, 22, 31, 19, 7, 8]
Offshore Wind	[30, 21, 22, 31, 19, 7, 8]
Solar Photovoltaic (PV)	[30, 32, 19, 33, 7, 8]
High-voltage direct current interconnection (HVDC)	[34, 7, 35]
Pumped hydro	[36, 19, 8]
Lead-acid battery	[37, 38]
Power system	
Hourly electricity demand	[39]
Hourly onshore/offshore wind/solar availability	[30, 40, 41]
Capacity reserve for intermittent renewables	[42]
Minimum system inertia	[43]
CO_2 emission target	[44]
Carbon intensity of imported electricity	[45]
Price of imported electricity	[46]
Carbon price	[47]
Transmission & distribution losses	[48, 49, 50]
Value of lost load	[51]
Carbon transport & storage cost	[13]
Fuel cost	
Coal	[52]
Natural gas	[52]
Biomass	[53]
Uranium (UO_2 fuel)	[54]

Supplementary Table 2: Data sources for parametrisation of the ESO-X model inputs. Most source contain relevant data to different technical and economic features.

To caption of Supplementary Table 2:

- The exact input files for the model evaluations for this work are available at Zenodo via *DOI 10.5281/zenodo.1048943* [55] and *DOI 10.5281/zenodo.1212298* [56]. The data source was created in an effort to provide a validated and transparent reference for power systems modelling data, however, no guarantee is given for its correctness.
- Hourly electricity demand is averaged from half-hourly to hourly values [39].
- Due to data availability and experience, lead-acid batteries are chosen as case study for this work. Lead-acid batteries are a favourable technology due to low capital cost and versatile grid-level applications (peak shaving, load shifting, spinning reserve, frequency and voltage control). However, low energy density and environmental challenges with lead disposal remain. However, currently sodium-sulfur batteries are dominating the market for grid-scale applications, and lithium-ion batteries are likely to enter grid-scale application [57].
- The CO_2 emission target is extrapolated from 2035 to 2050.
- The value for carbon intensity of imported electricity is set to 0.053 for t_{CO_2}/MWh France, 0.474_{CO_2}/MWh for Ireland and the Netherlands [45].

Supplementary Note 1

BECCS	Bioenergy with carbon capture and storage
CAPEX	capital expenditures
CCGT	Combined cycle gas turbine
CCS	Carbon capture and storage
CLC-CCS	Chemical looping combustion combined with carbon capture and storage
ESO	Electricity Systems Optimisation
ESO-X	Electricity Systems Optimisation with capacity expansion
ESO-XEL	Electricity Systems Optimisation with capacity expansion and endogenous technology learning
ESONE	Electricity Systems Optimisation with spatially granular capacity expansion
ESONE-XEL	Electricity Systems Optimisation with spatially granular capacity expansion and endogenous technology learning
FR	France
HVDC	High-voltage direct current
IE	Ireland
IGCC	Integrated gasification combined cycle
Interconn.	High voltage electric interconnector
NL	The Netherlands
OCGT	Open cycle gas turbine
OPEX	Operational expenditures
PostCCS	Post-combustion carbon capture and storage
PV	Photovoltaic
SMR	Small modular nuclear reactor
ST	Super technology

TRL	Technology readiness level
TSC	Total system cost
VoLL	Value of Lost Load

Supplementary Note 2

The following list summarises some of the assumptions taken as part of the model building process:

- We take the perspective of a monopolistic system planner.
- We assume perfect and imperfect foresight over the planning horizon. The underlying modelling technique is described in supplementary note 7.
- We assume electricity demand and electricity import prices to be inelastic.
- Uncertainty in the input parameters is not considered. The model is deterministic.
- In model version ESONE and ESONE-XEL the electric transmission network is modelled as HVDC lines connecting the zone centroids. In the ESO, ESO-X, ESO-XEL model version, the electric transmission system is represented as a single-node network. Overall transmission losses are, however, considered.
- In the ESO-XEL, ESONE-XEL model version, we assume that endogenous technological change is reflected in the capital cost of the power plant only and are based on global experience until today. Learning (endogenous change) of technology performance parameters is not assumed.
- CO_2 accounting of HVDC interconnection capacity is based on average carbon intensity levels for electricity generation in the connected power networks (i.e., 0.053 t_{CO_2}/MWh France and the Netherlands, 0.474 for Ireland) [58].

Supplementary Note 3

The following nomenclature and model formulation consisting of constraints 7-34 and objective function 40 refer to the ESO-X model.

Nomenclature

Symbol	**Unit**	**Description**
Sets		
a	yrs	planning periods, $a \in A = \{1, ..., A_{end}\}$
t	h	time periods, $t \in T = \{1, ..., T_{end}\}$
c	-	clusters of representative days of each year, $c \in C = \{1, ..., C_{end}\}$
i	-	technologies, $i \in I = \{1, ..., I_{end}\}$
ig	-	power generating technologies, $ig \subseteq I$
ic	-	conventional generating technologies, $ic \subseteq I$
ir	-	intermittent renewable technologies, $ir \subseteq I$
is	-	storage technologies, $is \subseteq I$
il	-	technologies for which learning rate is applied, $il \subseteq I$
l	-	line segments for piecewise linear function
Parameters		
Δ_a	yrs	step width planning years
$DIni_i$	-	number of available units of technology i for $a = 1$

$DMax_i$	-	maximum number of available units of technology i for $a = 1$
Des_i	MW/unit	nominal capacity per unit of technology i
BR_i	unit/yr	build rate of technology i
$MA_{i,a}$	-	maturity parameter, availability of technology i in year a
$LTIni_i$	yrs	lifetime of initial capacity of technology i for $a = 1$
LT_i	yrs	lifetime of technology i
TL	%	losses in transmission network
$TE_{i,*}$	various	features of technology i,
where * is:		
$Pmin$	%-MW	minimum power output
$Pmax$	%-MW	maximum power output
$Cmax$	%-MW	maximum capacity provision
RP	%-MW	reserve potential, ability factor to provide reserve capacity $\in = \{0, 1\}$
IP	%-MW	inertia potential, ability factor to provide inertial services $\in = \{0, 1\}$
Ems	t_{CO_2}/MWh	emission rate.
$CAPEX_i$	£/unit	investment costs of technology i
$OPEX_{i,a}$	£/MWh	operational costs of technology i in year a
$OPEXSU_i$	£/MWh	start-up costs of technology i
$OPEXNL_i$	£/h	fixed operational costs of technology i when operating in any mode
$ImpElecPr_{c,t}$	£/MWh	electricity import price
UT_{ig}	h	minimum up-time for technology ig
DT_{ig}	h	minimum down-time for technology ig
$SEta_{is}$	%-MWh	storage round-trip efficiency
$SDur_{is}$	h	maximum storage duration
$SOCMin_{is}$	%-MW	minimum storage inventory level
$SOCMax_{is}$	%-MW	maximum storage inventory level
$AV_{ir,c,t}$	%-MW	availability factor of technology ir in cluster c at hour t
$SD_{c,t,a}$	MWh	system electricity demand in year a in cluster c at hour t
UD	MWh	maximum level of unmet electricity demand in any year a
PL_a	MW	peak load over time horizon T in each year a
CM	%-MW	capacity margin
RM	%-MW	absolute reserve margin
WR	%-MW	dynamic reserve for wind power generation
SI	MW.s	minimum system inertia demand
SE_a	t_{CO_2}	system emission target in year a
$VoLL$	£/MWh	Value of Lost Load
$Disc_a$	-	discount factor $(1 + r)^a$ in year a
WF_c	-	weighting factor for clusters c
$Xlo_{il,l}$	MW	lower segment x-value of cumulative capacity of piecewise linear cost function
$Xup_{il,l}$	MW	upper segment x-value

$Ylo_{il,l}$	MW	lower segment y-value of cumulative CAPEX
$Yup_{il,l}$	MW	upper segment y-value
Variables		
tsc	£	total system cost
$e_{ig,a,c,t}$	t_{CO_2}	emission caused by technology ig in year a at hour t of cluster c
Positive Variables		
$p_{ig,a,c,t}$	MWh	energy output of technology i in year a in hour t of cluster c
$p2d_{ig,a,c,t}$	MWh	energy to demand
$p2s_{ig,a,c,t}$	MWh	energy to grid-level storage
$p2is_{is,a,c,t}$	MWh	energy to storage technology is
$r_{ig,a,c,t}$	MW	reserve capacity provided by technology ig
$s_{is,a,c,t}$	MWh	effective state of charge of technology is at the end of time period t
$s2d_{is,a,c,t}$	MWh	energy from storage to demand
$s2r_{is,a,c,t}$	MW	reserve capacity provided by technology is
$slak_{a,c,t}$	MWh	slack variable for lost load
$emslak_{a,c,t}$	t_{CO_2}	slack variable for emissions
$xs_{il,a,l}$	MW	position for technology i in year a on line segment l
$y_{il,a}$	£	cumulative CAPEX for technology i in year a
Integer Variables		
$b_{i,a}$	-	number of new built units of technology i in year a
$d_{i,}$	-	number of units of technology i operational in year a, cumulative
$n_{ig,a,c,t}$	-	number of units of technology ig operating in year a at hour t of cluster c
$o_{is,a,c,t}$	-	number of units of storage technology is operating in year a at hour t of cluster c
$u_{ig,a,c,t}$	-	number of units of technology ig starting up in year a at time t of cluster c
$w_{ig,a,c,t}$	-	number of units of technology ig turning down in year a at time t of cluster c
Binary Variables		
$\rho_{il,a,l}$	-	1, if cumulative CAPEX of technology il in year a on line segment l

System design constraints

$$d_{i,a} = DIni_i \qquad \forall i, a = 1 \qquad (1)$$
$$b_{i,a} \leq BR_i \, MA_{i,a} \, \Delta_a \qquad \forall i, a > 1 \qquad (2)$$
$$d_{i,a} \leq DMax_i \qquad \forall i, a \qquad (3)$$
$$d_{i,a} = d_{i,a-1} - b_{i,a-\frac{LTIni_i}{\Delta_a}} + b_{i,a} \qquad \forall i, a \leq \frac{LTIni_i}{\Delta_a} + 1 \qquad (4)$$
$$d_{i,a} = d_{i,a-1} + b_{i,a} \qquad \forall i, \frac{LTIni_i}{\Delta_a} + 1 < a \leq \frac{LT_i}{\Delta_a} + 1 \qquad (5)$$
$$d_{i,a} = d_{i,a-1} - b_{i,a-\frac{LT_i}{\Delta_a}} + b_{i,a} \qquad \forall i, a > \frac{LT_i}{\Delta_a} + 1 \qquad (6)$$

Unit commitment variables

$$n_{ig,a,c,t} \leq d_{ig,a} \qquad \forall ig, a, c, t \qquad (7)$$
$$o_{is,a,c,t} \leq d_{is,a} \qquad \forall is, a, c, t \qquad (8)$$

System wide power balance, security, and emission constraint

Constraint 13 is part of the model formulation only if enforced decarbonisation is desired. Otherwise, constraint 13 is relaxed and decarbonisation is driven by the carbon price (included in the parameter $OPEX_{ig,a}$) only.

$$\sum_{ig} p2d_{ig,a,c,t} + \sum_{is} s2d_{is,a,c,t} = SD_{c,t,a} \, (1 + TL) - slak_{a,c,t} \qquad \forall a, c, t \qquad (9)$$
$$\sum_{i} d_{i,a} \, Des_i \, TE_{i,\mathsf{Cmax}} \geq PL_a \, (1 + CM) \qquad \forall a, t \qquad (10)$$
$$\sum_{ig} r_{ig,a,c,t} \, TE_{ig,\mathsf{RP}} + \sum_{is} s2r_{is,a,c,t} \, TE_{is,\mathsf{RP}}$$
$$\geq SD_{c,t,a} \, RM + \sum_{ir} p2d_{ir,a,c,t} \, WR \qquad \forall a, c, t \qquad (11)$$
$$\sum_{ig} n_{ig,a,c,t} \, Des_{ig} \, TE_{ig,\mathsf{IP}} \geq SI \qquad \forall a, c, t \qquad (12)$$
$$\sum_{ig,c,t} (e_{ig,a,c,t} - emslak_{a,c,t}) \, WF_c \leq SE_a \qquad \forall a \qquad (13)$$
$$\sum_{c,t} slak_{a,c,t} \, WF_c \leq UD \sum_{t} SD_{c,t,a} \qquad \forall a \qquad (14)$$

Technology specific unit commitment, power and ancillary service constraints

$$p_{ic,a,c,t} \geq n_{ic,a,c,t}\, Des_{ic}\, TE_{ic,\mathsf{Pmin}} \qquad \forall ic, a, c, t \tag{15}$$
$$p_{ig,a,c,t} + r_{ig,a,c,t} \leq n_{ig,a,c,t}\, Des_{ig}\, TE_{ig,\mathsf{Pmax}} \qquad \forall ig, a, c, t \tag{16}$$
$$p_{ig,a,c,t} = p2d_{ig,a,c,t} + p2s_{ig,a,c,t} \qquad \forall ig, a, c, t \tag{17}$$
$$p_{ir,a,c,t} \geq n_{ir,a,c,t}\, Des_{ir}\, TE_{ir,\mathsf{Pmin}}\, AV_{ir,c,t} \qquad \forall ir^{\setminus} InterImp, a, c, t \tag{18}$$
$$p_{ir,a,c,t} + r_{ir,a,c,t} \leq n_{ir,a,c,t}\, Des_{ir}\, AV_{ir,c,t} \qquad \forall ir^{\setminus} InterImp, a, c, t \tag{19}$$
$$e_{ig,a,c,t} = (p_{ig,a,c,t} + r_{ig,a,c,t})\, TE_{ig,\mathsf{Ems}} \qquad \forall ig, a, c, t \tag{20}$$
$$\sum_{c,t} p_{ic,a,c,t}\, WF_c/8760 \geq TE_{ic,\mathsf{UtilMin}}\, d_{ic,a}\, Des_{ic} \qquad \forall ic, 1 < a < T_{end} \tag{21}$$

Unit up-time and down-time constraints

$$u_{ig,a,c,t} \geq n_{ig,a,c,t} - n_{ig,a,c,t-1} \qquad \forall ig, a, c, t \tag{22}$$
$$w_{ig,a,c,t} \geq n_{ig,a,c,t-1} - n_{ig,a,c,t} \qquad \forall ig, a, c, t \tag{23}$$
$$u_{ig,a,c,t} \leq n_{ig,a,c,\tau} \qquad \forall ig, a, c, \tau = t + t' - 1, t' \leq UT_{ig} \tag{24}$$
$$w_{ig,a,c,t} \leq d_{ig,a} - n_{ig,a,c,\tau} \qquad \forall ig, a, c, \tau = t + t' - 1, t' \leq DT_{ig} \tag{25}$$

Storage operation constraints

$$s2d_{is,a,c,t} + s2r_{is,a,c,t} \geq o_{is,a,c,t}\, Des_{is}\, TE_{is,\mathsf{Pmin}} \qquad \forall is, a, c, t \tag{26}$$
$$s2d_{is,a,c,t} + s2r_{is,a,c,t} \leq o_{is,a,c,t}\, Des_{is} \qquad \forall is, a, c, t \tag{27}$$
$$s2d_{is,a,c,t} + s2r_{is,a,c,t} \leq s_{is,a,c,t}\, SEta_{is} \qquad \forall is, a, c, t \tag{28}$$
$$s_{is,a,c,t} = Des_{is}\, SOCIni_{is}\, SDur_{is} \qquad \forall is, a, c, t = 1 \tag{29}$$
$$s_{is,a,c,t} \leq o_{is,a,c,t}\, Des_{is}\, SOCMax_{is}\, SDur_{is} \qquad \forall is, a, c, t \tag{30}$$
$$s_{is,a,c,t} \geq o_{is,a,c,t}\, Des_{is}\, SOCMin_{is}\, SDur_{is} \qquad \forall is, a, c, t > SDur_{is} \tag{31}$$
$$\sum_{ig} p2s_{ig,a,c,t} = \sum_{is} p2is_{is,a,c,t} \qquad \forall a, t \tag{32}$$
$$p2is_{is,a,c,t} \leq o_{is,a,c,t}\, Des_{is} \qquad \forall is, a, c, t \tag{33}$$
$$\begin{aligned} s_{is,a,c,t} = {} & s_{is,a,c,t-1} - s2d_{is,a,c,t} \\ & + \sum_{is} p2is_{is,a,c,t}\, SEta_{is} \qquad \forall is, a, c, t > 1 \end{aligned} \tag{34}$$

Endogenous cost reduction

$$\sum_{l} \rho_{il,a,l} = 1 \qquad \forall il, a \tag{35}$$

$$xs_{il,a,l} \geq Xlo_{il,l}\, \rho_{il,a,l} \qquad \forall il, a, l \tag{36}$$

$$xs_{il,a,l} \leq Xup_{il,l}\, \rho_{il,a,l} \qquad \forall il, a, l \tag{37}$$

$$\sum_{a'=1}^{a} b_{il,a'} = \sum_{l} xs_{il,a,l} \qquad \forall il, a, a' \leq a \tag{38}$$

$$\begin{aligned} y_{il,a} = \sum_{l} & Ylo_{il,l} \\ & + \rho_{il,a,l} Slope_{il,l}\,(xs_{il,a,l} - Xlo_{il,l}\, \rho_{il,a,l}) \qquad \forall il, a \end{aligned} \tag{39}$$

Objective function

$$\begin{aligned} & minimise\{tsc\} \\ & tsc = \sum_{i \in I \setminus il,a} CAPEX_i\, b_{i,a}\, Des_i / Disc_a \quad + \sum_{il,a} (y_{il,a} - y_{il,a-1}) / Disc_a \\ & \quad + \sum_{ig,a,c,t} (u_{ig,a,c,t}\, OPEXSU_{ig}\, WF_c) / Disc_a \\ & \quad + \sum_{ig,a,c,t} (OPEX_{ig,a}\, p_{ig,a,c,t}\, WF_c + OPEXNL_{ig}\, n_{ig,a,c,t}\, WF_c) / Disc_a \\ & \quad + \sum_{is,a,t} (OPEX_{is,a}\, s2d_{ig,a,c,t}\, WF_c + OPEXNL_{is}\, o_{is,a,c,t}\, WF_c) / Disc_a \\ & \quad + \sum_{i = InterImp,a,t} ImpElecPr_t\, p2d_{i,a,c,t}\, WF_c / Disc_a \\ & \quad + \sum_{a,c,t} slak_{a,c,t}\, WF_c\, VoLL \\ & (\quad + \sum_{a,c,t} emslak_{a,c,t}\, WF_c\, EPenalty \quad) \end{aligned} \tag{40}$$

Supplementary Note 4

We parametrise two "super technologies":

1. Chemical Looping Combustion (CLC) in a Natural Gas Combined Cycle (NGCC) in combination with Carbon Capture and Storage (CCS), in the following referred to as CLC-CCS,
2. Small modular nuclear reactor (SMR).

For both type of technologies some salient parameters are presented in supplementary table 3 below. The full set of parameters can be found in the online documentation at Zenodo via *DOI 10.5281/zenodo.1048943* [55] and *DOI 10.5281/zenodo.1212298* [56].

Parameter	Unit	NGCC-CLC	SMR
Efficiency	$\%_{HHV}$	46.8	28
Unit size	MW/unit	500	50
CAPEX	$£_{2015}$/kW	1,066	3,567
OPEX_{fixed}	$£_{2015}$/MWh	2.46	3
$\text{OPEX}_{fuel,CO_2tax,T\&S}$	$£_{2015}$/MWh	37.8	9.29
$\text{OPEX}_{start-up}$	$£_{2015}$/start	79,564	4,000
Economic lifetime	years	40	50
Construction time	years	5	2
Carbon intensity (emitted)	t_{CO_2}/MWh	0	0
Carbon intensity (captures)	t_{CO_2}/MWh	0.386	0
Minimum stable generation	%	40	20
Maximum power output	%	90	95
Capacity credit	%	90	96
Inertia potential	MW.s/MW	10	10
Reserve potential	%-MW	100	100
Minimum up time	h	4	1
Minimum down time	h	1	1

Supplementary Table 3: Parametrisation of "super technology" in ESO-X model as NGCC-CLC [59, 60, 61, 18] and small modular nuclear reactor (SMR) [62, 63, 64, 65, 1, 66]. The inertia potential is an approximation representing the ability of a power unit to provide inertial service, electric power (stored in rotating mass, typically in direct synchronous generators) to ensure against frequency excursion [11]. The reserve potential is an approximation representing the ability of a power unit to provide its capacity reserve services.

Supplementary Note 5

The infrastructure and supply chain aspects of large-scale CCS equipped power generation capacity are likely to play a significant role on the project economics. To approximate these effects we allocate the expected additional cost for the development of a CO_2 transport and storage infrastructure to the power plants capital cost. However, as deployment increases these infrastructure cost are likely to reduce. Hence, we model a CLC-CCS power plants capital cost in form of an endogenous piecewise linear cost curve. Costs are assumed to reduce from a value twice the actual cost estimate (see supplementary table 3), reduction factor is set to reduce cost upon deployment accounting for project cost reduction once infrastructure is in place. Equation 41 determines the the costs C_n of the n^{th} capacity unit as a function of the initial cost C_{Ini}, the cumulative installed capacity up to the n^{th} unit x_n, and the cost reduction rate factor bLR, analogous to the cost learning theory [8].

$$C_n = C_{Ini} \cdot x_n^{bLR} \tag{41}$$

A price floor ensures that cost do not fall below the cost estimate in supplementary table 3. We do not consider technological learning effects due to research and development, manufacturing advancement, etc., as discussed in [67]. Supplementary figure 4 visualises the cost reduction curves for CLC-CCS capacity deployment. The left hand side graph represents the unit capital cost as a function of cumulative capacity deployment. The right hand side graph illustrates the piecewise linear curve (diamonds), and the piecewise linear cumulative cost curve (squares) as integrated into the modelling framework via constraints 35 - 39, see supplementary note 3.

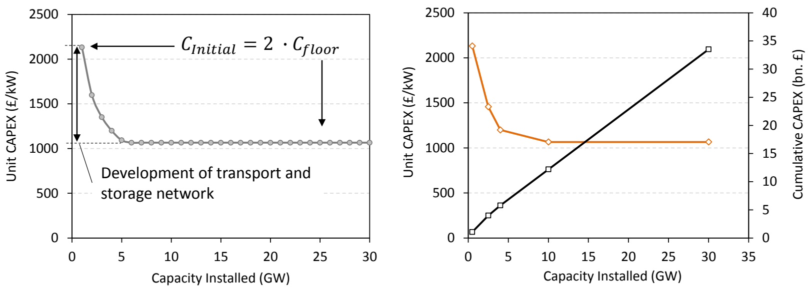

Supplementary Figure 4: Cost reduction assumptions for CLC-CCS capacity deployment (left), as piecewise linear function (right, diamonds), as piecewise cumulative cost curve (right, squares).

Supplementary Note 6

The ESO models are implemented in GAMS 24.8.3 [68] and solved with CPLEX 12.3 [69] on an Intel i7-4770 CPU, 3.4 GHz machine with 8 GB RAM using 8 threads. All model runs are solved to an optimality gap of 3 %.

Hourly Data Processing and Relaxation

In order to reduce computational solution times two main solution strategies are applied to the ESO model input data and formulation presented in section supplementary note 3.

1. K-means data clustering [18] with "energy-preserving" profiling [67],
2. Relaxation of integer scheduling constraints [70, 71, 72].

Heuberger et al. [73, 67] provides detail on both solution strategies and explicitly examines their implication on technology-specific and system-level results. The overall error in the objective function value (total system cost, tsc) ranges between -1.7 % to +2.5 % for 21 to 11 clusters with 24 hours each representing the 8760 hours of the year over a 35 year time period (2015-2050). The intra-day operation of power generation and energy storage units is not affected by the cluster algorithm. However, long-term or seasonal energy storage operation cannot be modelled via this approach as time continuity between the clusters is not preserved. Areas of further research could be cluster length as well as clustering in combination with seasonal energy storage options [74]. For all presented results in the main paper and in the supplementary document the hourly time dependent data is compressed to 11 clusters, the integer scheduling variables $n_{ig,a,c,t}$, $o_{is,a,c,t}$, $u_{ig,a,c,t}$, and $w_{ig,a,c,t}$ are relaxed, and the integer scheduling constraints are replaced with their convex hull reformulation (constraints 22-22). Supplementary figure 9 and 10 in section supplementary discussion visualise the hourly operation for the 11 representative clusters.

Supplementary Note 7

Review of existing work

Early work by Levin et al. initiated the discussion on myopic versus full time horizon planning in large-scale energy system models [75]. It was found that with simplified conditions (such as no start-up cost, no economies of scale, all power plants are dispatchable) both approaches can lead to equal results. More recently, imperfect foresight conditions have been studied in an effort to improve the assumptions in energy systems models. There are models which were originally formulated under myopic conditions such as SAGE [76], and IKARUS with five yearly time steps [77]. The BLUE model additionally accounts for the effect of multiple sector-specific actors [78, 79]. The IMACLIM-R model recursively updates system and technology parameters; imperfect foresight and imperfect competition represent "second-best" economy characteristics [80].

Analysis with the MESSAGE integrated assessment model find that myopic approaches show lower levels of early investments and result in higher carbon intensity levels by 2050 and 2100 [81]. Similar analysis with the PERSEUS-NET and UKTM model and argue that both approaches can be suitable for different research questions [82, 83]. It was shown that myopic versus perfect foresight approaches result in structurally different future power systems. Again early investments in low-carbon technologies are delayed and total system cost to achieve CO_2 emission reductions are greater under myopic planning [83].

Rolling horizon optimisation

In this work we contrast anticipatory planning by extending the perfect foresight ESO model framework according to section supplementary note 3 with an rolling-horizon solution algorithm representing myopic planning. Supplementary figure 5 illustrates the two approaches and their key differences. In the perfect foresight form, the ESO model is solved in a single instance for the full planning horizon (time steps a in the model formulation, for illustrative reasons time steps t in supplementary figure 5 not according to the model formulation). All parameter values (*e.g.*, future cost, when a technology becomes available) from the first to the last time step are "known" during the solution process, and all constraints are active.

Under imperfect or myopic foresight conditions, the model is solved iteratively where future parameter values are "unknown" and only a subset on constraints is active while future constraints are relaxed. As the algorithm proceeds, the parameter data is updated (*e.g.*, a disruptive technological advancement, a change in cost or performance, or system-level ambition can be introduced), the subset of decision variables from the previous iteration are fixed, and the model is solved for the ensuing set of active constraints. The algorithm terminates if the model is solved for all time steps and all decisions variable values have been fixed. In this work we choose an iteration step length of one planning time step which is equivalent to a five year time step.

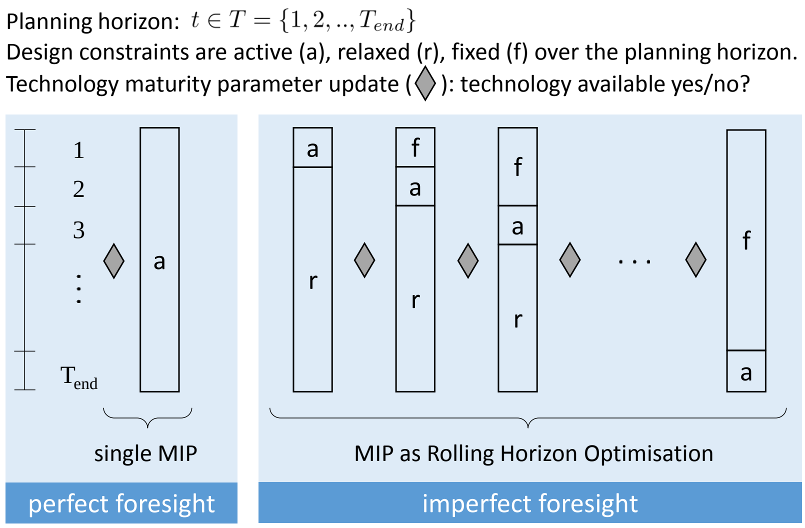

Supplementary Figure 5: Solution strategy for a perfect foresight model (left) and myopic foresight (right). The initial vs. iterative update of the technology maturity parameter ($\in [0, 1]$), which determines a technology's readiness to be deployed in a given planning horizon a, enables the representation of an imperfect foresight with respect to technology availability.

Supplementary Discussion

Scenarios with Small Modular Nuclear Reactors and increased availability battery storage as "super technology"

To assess the sensitivity of the results of the main paper, we analyse scenarios 1 and 2 for the integration possibility of SMRs, SMRs with a 10 % learning rate (*i.e.*, at each doubling of cumulative installed capacity capital cost reduce by 10 %), and increased availability of grid-scale lead-acid battery storage. Battery storage is available in all "go" scenarios, however, the rate of deployment and the maximum capacity installation is limited (500 MW/year, 3 GW by 2050, based on [44]). In the high build rate (BR) scenario for lead-acid batteries, as much as 1 GW can be added per year with an upper bound of 30 GW by 2050 (supplementary figure 6, right).

In a "wait" scenario (2b) where instead of CLC-CCS SMR capacity becomes available as super technology in 2035, their deployment is not part of the optimal least-cost solution. This is mainly due to the high investment cost of the SMR technology (£3567/kW for a first-of-a-kind power plant). Equally, if technology cost learning for SMR units at a 10 % learning rate are taken into consideration, SMR deployment remains uneconomical under the given scenario conditions.

We modify the "go" scenario 1b which initially does not consider disruptive technology change to include this possibility. Supplementary figure 6 visualises the integration of CLC-CCS, SMR, and high available large-scale lead-acid batteries under committed climate action (analogous to 1b). In this case, SMR capacity is valuable and deployment gradually increases to 9.4 GW by 2050 (supplementary figure 6, middle). The relatively high capital cost, £3567/kW compared to £2132/kW - £1066/kW for CLC-CCS, however, result in lower deployment levels compared to CLC-CCS (19.5 GW by 2050). The

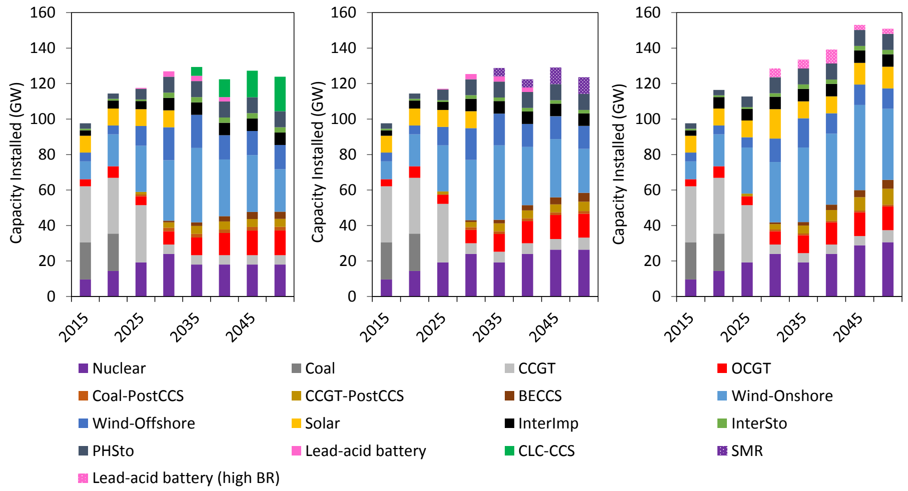

Supplementary Figure 6: Optimal capacity mix with super technology integration CLC-CCS (left) and SMR (middle), and increased deployment (high build rate (BR)) of lead-acid battery capacity (right). Scenario analogous to 1b with respective super technology availability.

costs for CLC-CCS are assumed to reduce upon deployment accounting for the development of the CO_2 transport and storage network, see section supplementary note 5. If SMR capacity cost are modelled with a 10 % learning rate deployment increases to 14.55 GW by 2050. As capital cost reduce upon deployment, further capacity additions become more profitable (not shown in supplementary figure 6).

The increased availability of lead-acid batteries for grid-level integration proves valuable and allows a greater share of intermittent renewable penetration between 2040 and 2050 compared to CLC-CCS and SMR integration. By 2040 7.9 GW of grid-level energy storage would be economically optimal. Towards 2050 the storage capacity stock reduces due to the end of lifetime of existing storage capacity to 2.9 GW in 2050. Additionally, as the end of the planning horizon is reached, no new capacity is build for years post-2050. So called "end-of-horizon-effects" can be circumvented by accounting for expected cost/revenues beyond the end of the planning horizon, however are outside the scope of this work.

Supplementary figure 6 compares for the four technology integration options, cumulative total system cost (TSC), the difference in annual TSC between to CLC-CCS, and system-wide carbon intensity. SMR and increased lead-acid battery integration lead to higher cumulative TSC by 2050 (supplementary figure 7, left). The annual TSC comparison reveals that in 2030 the increased integration of battery storage capacity (5 GW are installed) reduces costs significantly. Beyond 2030, however, the power system based on high levels of intermittent renewables and storage is up to 150 % more costly than a power system with the super technology CLC-CCS. Similarly, SMR integration shows significantly higher cost upon deployment beyond 2035. The SMR integration case considering technology cost learning shows lower TSC difference compared to SMR with constant cost as deployment increases. Given the enforced decarbonisation of the power sector in these scenarios the carbon intensity level can be reduced equally with all three technology options.

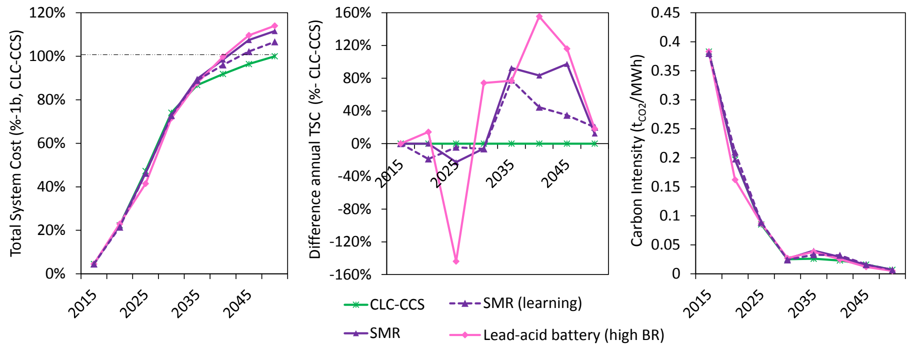

Supplementary Figure 7: For super technology integration CLC-CCS and SMR, SMR considering a 10 % learning rate, and increased deployment (high build rate (BR)) of lead-acid battery capacity, comparison of cumulative total system cost (TSC) (left), difference in TSC compared to CLC-CCS (middle), system-wide carbon intensity (right).

Supplementary table 4 summarises the optimal levels of capacity installed as output of the ESO-XEL model runs according to scenarios 1b and 2b. The amount of battery capacity installed reduced in both scenarios from 2040 to 2050 due to end of lifetime constraints and an increase in interconnection capacity which is able to provide flexibility to the power system.

Technology	2b		1b	
	2040	2050	2040	2050
CLC-CCS	10	15	10	19.5
SMR	0	0	4.65	9.4
SMR (learning)	0	0	9.55	14.55
Battery	6.3	1.2	7.9	2.9

Supplementary Table 4: Optimal deployment level of different "unicorn technology" options CLC-CCS, SMR, SMR with 10 % learning rate, and increased availability of lead-acid batteries.

Additional sensitivity analysis

To evaluate the validity of the main results and gain further insights into the strengths and limitations of the prosed modelling approach we perform a sensitivity analysis on two core system level parameter, electricity demand and fuel prices.

Electricity demand

Future demand is one of the key uncertainties in energy systems planning [84]. In the UK, the Committee on Climate Change (CCC) [85] estimates a range of 50-135 % power demand increase by 2050 from 2015 levels depending on different electrification pathways (*e.g.*, sector integration, electrification of heat and transport). The presented base scenarios in the main paper and additional scenarios in the supplementary information refer to a annual demand increase of 1 % per year, equivalent to 41 % total increase from 2015 to 2050. This section presents an analysis for a "high demand" scenario which is chosen at a medium level of the CCC's estimates and represents a demand increase of 2 % per year, or a 95 % increase from 2015 to 2050. Although electricity demand patterns are likely to be affected by the changing energy system landscape [86], for the sake of simplicity we assume that in both cases the hourly demand profiles remain the same over the planning horizon (see supplementary table 2).

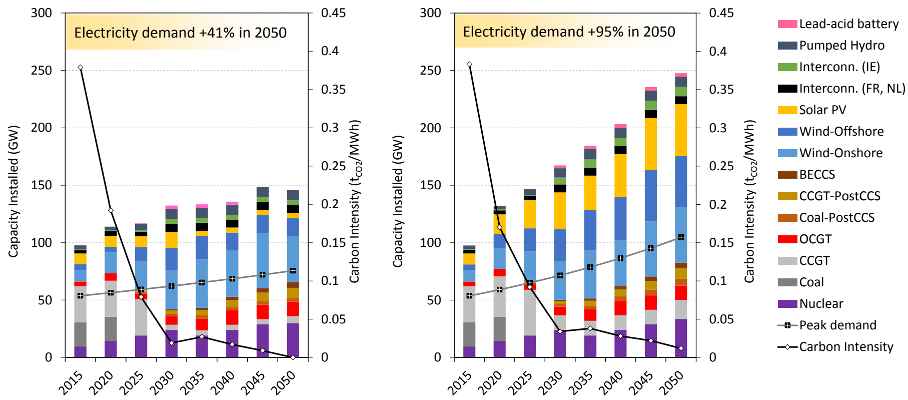

Supplementary Figure 8: Capacity expansion for base case 1b (left) and increased electricity system demand (right) such that annual demand in 2050 is 95 % greater compared to 2015; corresponding peak demand (input parameter) and carbon intensity level (output).

Supplementary figure 8 compares the two demand scenarios and visualises the annual peak demand in relation to the total installed capacity. Under accelerated demand increase (supplementary figure 8, right) and due to the 2050 decarbonisation target, all low-carbon technologies (*i.e.*, nuclear, CCS-equipped power plants, wind, solar) are deployed to their maximum level in each planning period. Hence, all discrete variables describing capacity build-up ($b_{i,a}$) are set to their upper bound value (see constraint 2) in supplementary note 3), which is based on historically observed maximum build rates in the UK [87] (here for scenario type 1, see supplementary table 1).

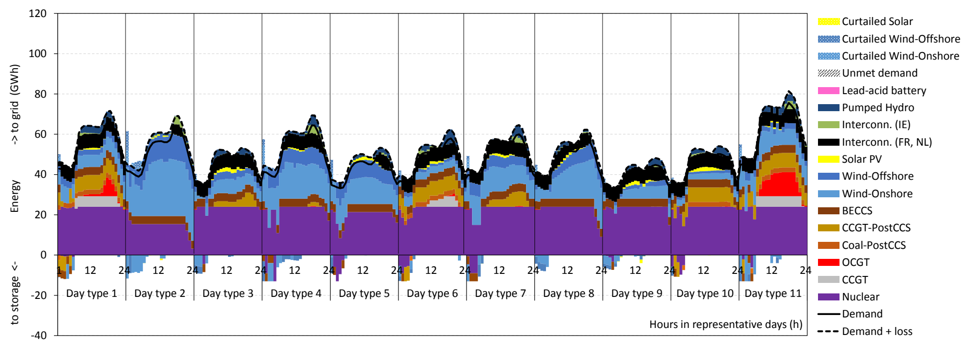

Supplementary Figure 9: Hourly operational profile for base scenario 1b in 2050 showing the aggregate of all units per technology type for each representative day as determined via the proposed clustering approach in supplementary note 6.

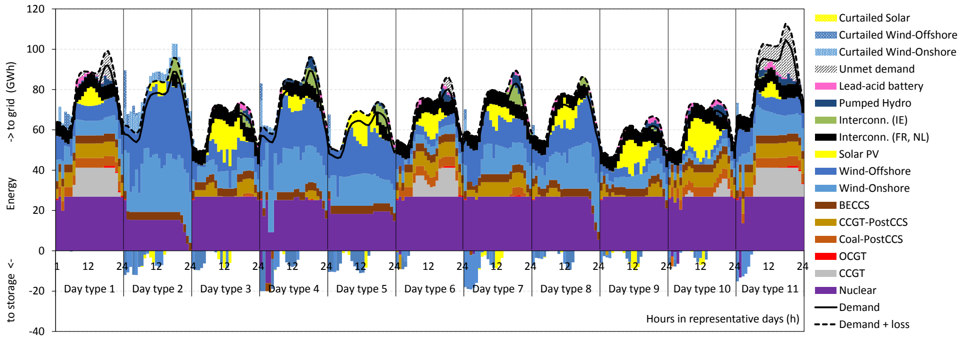

Supplementary Figure 10: Hourly operational profile for scenario 1b in 2050 under high electricity demand showing the aggregate of all units per technology type for each representative day as determined via the proposed clustering approach in supplementary note 6.

Supplementary figures 9 and 10 visualise the hourly power generation and storage charging and discharging patterns for the base and high demand scenario in 2050, respectively. The higher share of intermittent renewable power generation from onshore wind, offshore wind, and, especially during mid-day, from solar PV capacity in the high demand scenario lead to steeper ramp rates for the dispatchable power plants, *i.e.*, CCGT, and CCS-equipped (compare for example representative day type 6 and 12).

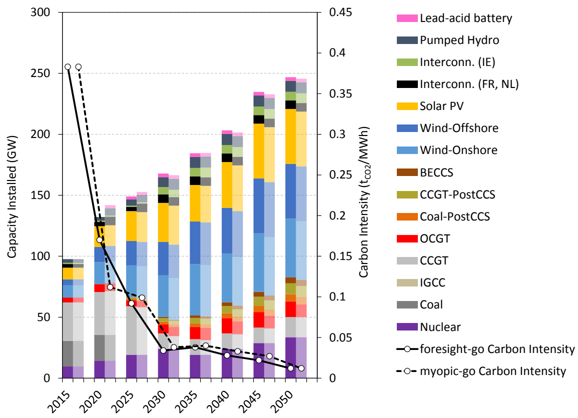

Supplementary Figure 11: Capacity expansion for high demand scenario with perfect foresight (left, full coloured bars) and myopic foresight (right, shaded bars); corresponding carbon intensity levels.

Supplementary figure 11 visualises the effect of perfect foresight versus myopic planning under the high demand scenario, analogous to figure 2 (right hand side) in the main paper. The results show the same trend to the base case in the initial planning years up to 2025 where more capacity is built early on. In the high demand case, we see an increased deployment of energy storage and flexible unabated gas-fired power plants. The perfect foresight option shows a more infrastructurally efficient capacity stack. Additional capacity is built in later planning years when this is, from an investment perspective, more favourable due to a higher discount rate. In the myopic case, "corrective action" is taken in later planning periods where less capacity is built compared to the perfect foresight option. Due to the crucial role of the build rate parameter [67], the effects of myopic and perfect foresight planning on the capacity mix are not directly comparable to the reference case of the main paper.

From a cost perspective, the myopic case is sub-optimal compared to the perfect foresight case, resulting in overall 9 % greater total system cost (TSC) in 2050 (supplementary figure 12, panel b). In years 2015-2025, investment costs are higher in the myopic case when unabated CCGT, pumped hydro, and battery storage units are being built.

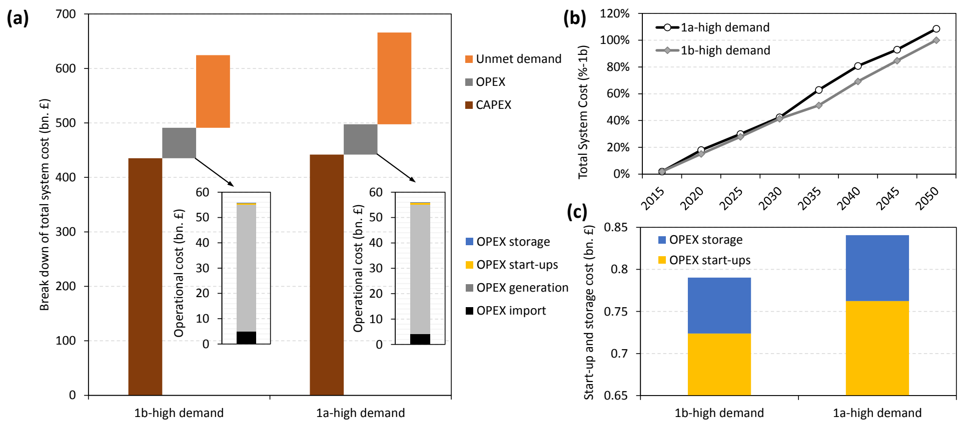

Supplementary Figure 12: For the high demand scenario, (panel a) breakdown of cumulative total system cost (TSC) from 2015 to 2050 for perfect foresight (1b) and myopic planning (1a); (panel b) cumulative TSC over planning time horizon; (panel c) start-up and energy storage cost as selected zoom-in to breakdown of operational expenses (OPEX) from embedded figures in panel a.

Supplementary figure 12 panel a visualises the breakdown of the cumulative TSC from 2015 to 2050 for the two foresight scenarios. Capital expenditures and costs associated with electricity demand not being met (*i.e.*, "lost load" is penalised by the so called Value of Lost Load (parameter $VoLL$) in the objective function 40, and limited to a maximum level of 0.05 % of annual electricity demand per year in constraint 14) are greater in the myopic case. The level of unmet demand reaches 0.046 % in 2035, whereas under perfect foresight planning conditions this level is reached only in year 2040. For comparison, the scenarios considering the base case electricity demand increase show marginal levels of unmet demand below 0.001 % in any planning year. The level of higher operational cost due to increased cycling (shut down and start-up) operation from dispatchable power plants and energy storage units in the myopic case is visualised in supplementary figure 12 panel c.

Fuel price

In the scenarios presented in the main paper, and other additional scenarios in the supplementary information the future fossil fuel prices are based on "central" projections by the UK's former Department of Energy & Climate Change [52] (now subsumed into the Department of Business Energy & Industrial Strategy). Projections are only provided up to 2040, and are constant between 2030 and 2040. We have extrapolated the constant cost values up to 2050. In this section, we present an analysis based on the "high" scenario. Supplementary figure 13 panel a visualises the two projections for coal and natural gas prices.

Supplementary figure 13 panel b is analogous to figure 2 (left) of the main paper and visualises the effect of myopia and the disruptive event of a super technology becoming available for deployment in 2035. We find that fuel prices do not have significant effect on overall results. Trends observed in the main paper with respect to the capacity expansion plan are analogous in the high fuel price scenarios, 1b, 2a, 2b.

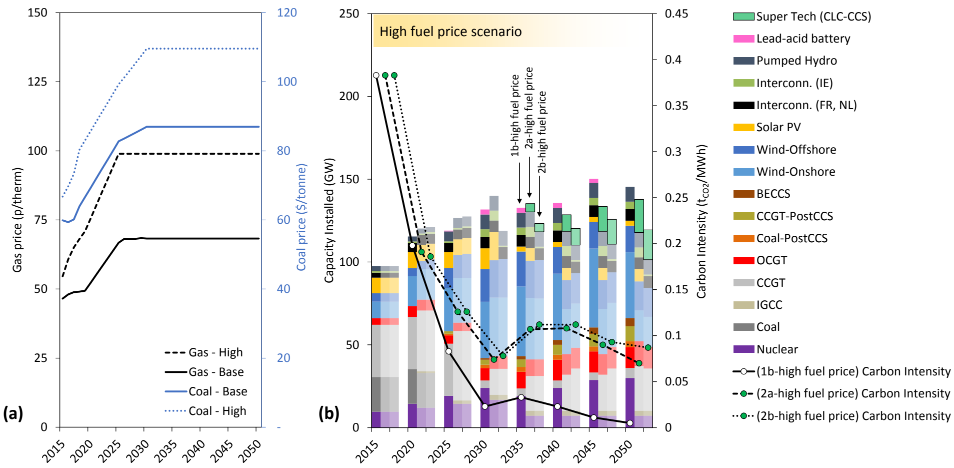

Supplementary Figure 13: Coal and gas fuel prices for base scenarios and high price scenario (panel a); capacity expansion and

Most noticeable in the carbon intensity curves for the different scenarios, the higher gas prices lead to lower gas-fired capacity installations (*i.e.*, in 2b: 25.5 GW CCGT and 13 GW OCGT compared to 26.25 GW and 14.8 GW in central case, respectively) and power generation in 2045 and 2050 compared to the scenarios with central fuel price (see figure 2 main paper).

Supplementary References

[1] A. Abdulla, I. L. Azevedo, and M. G. Morgan. Expert assessments of the cost of light water small modular reactors. *Proceedings of the National Academy of Sciences of the United States of America*, 110(24):9686–9691, 2013. ISSN 1091-6490. doi: 10.1073/pnas.1300195110. URL `http://www.pnas.org/content/110/24/9686.short`.

[2] T. Roulstone. SMRs will transform the nuclear industry, 2016. URL `https://tinyurl.com/y8m5cc8k`.

[3] A. Lokhov. Technical and Economic Aspects of Load Following with Nuclear Power Plants, 2011. URL `https://tinyurl.com/ycqqapkx`.

[4] J. Deutch and E. Moniz. Managing Large-Scale Penetration of Intermittent Renewables: An MIT Energy Initiative Symposium, 2011. URL https://tinyurl.com/ycdwpbce.

[5] Parsons Brinckerhoff. Electricity Generation Model - 2013 Update Of Non-Renewable Technologies: for Department of Energy and Climate Change, 2013. URL https://tinyurl.com/oqdn4hd.

[6] Mott MacDonald. UK Electricity Generation Costs Update, 2010. URL https://tinyurl.com/nhldhmv.

[7] Department of Energy & Climate Change. Electricity Generation Costs 2013, 2013. URL https://tinyurl.com/o25or2g.

[8] E. S. Rubin, I. M. L. Azevedo, P. Jaramillo, and S. Yeh. A review of learning rates for electricity supply technologies. *Energy Policy*, 86:198–218, 2015. doi: 10.1016/j.enpol.2015.06.011.

[9] R. Domenichini, L. Mancusoa, N. Ferrari, and J. Davison. Operating Flexibility of Power Plants with Carbon Capture and Storage (CCS). *Energy Procedia*, 37: 2727–2737, 2013. doi: 10.1016/j.egypro.2013.06.157. URL https://doi.org/10.1016/j.egypro.2013.06.157.

[10] N. Ferrari, L. Mancuso, and P. Cotone. Operating plant flexibility of power plants with CCS, 2012. URL https://tinyurl.com/yb76wyo6.

[11] A. Mullane, G. Bryans, and M. O'Malley. Kinetic energy and frequency response comparison for renewable generation systems. *International Conference on Future Power Systems*, 2005.

[12] D. Lew, G. Brinkman, E. Ibanez, A. Florita, M. Heaney, B.-M. Hodge, M. Hummon, and G. Stark. The Western Wind and Solar Integration Study Phase 2, 2013. URL http://www.nrel.gov/docs/fy13osti/55588.pdf.

[13] L. Mancuso and N. Ferrari. CO_2 capture at coal based power and hyrdoigen plants, 2014. URL https://tinyurl.com/jyw52w8.

[14] Department of Engineering & Public Policy. Integrated Environemtnal Control Model (IECM), 2015. URL http://www.cmu.edu/epp/iecm/index.html.

[15] D. Lunn. Technical Assessment of the Operation of Coal & Gas Fired Plants: Prepared for DECC, 2014. URL https://tinyurl.com/ybpa7wus.

[16] M. Finkenrath. Cost and Performance of Carbon Dioxide Capture from Power Generation, 2011. URL https://tinyurl.com/yarvpwbf.

[17] J. Chow, K. Ho, X. Du, H. S. Lee, and M. Pearson. Experience from extensive two-shift operation of 680MW coal/gas-fired units at castle peak power station - Hong Kong. *Operation, Maintenance and Material Issues*, 1(2), 2001. URL https://tinyurl.com/ycn653fn.

[18] R. Green, I. Staffell, and N. Vasilakos. Divide and Conquer? k-Means Clustering of Demand Data Allows Rapid and Accurate Simulations of the British Electricity System. *Transactions on Engineering Management*, 62(2):251–260, 2014. doi: 10.1109/TEM.2013.2284386.

[19] International Energy Agency. World Energy Investment Outlook: Special Report, 2014. URL `https://tinyurl.com/yap49crx`.

[20] N. Ceccarelli, M. van Leeuwen, T. Wolf, P. van Leeuwen, R. van der Vaart, W. Maas, and A. Ramos. Flexibility of low-CO_2 gas power plants: Integration of the CO_2 capture unit with CCGT operation. *Energy Procedia*, 36:1703–1726, 2014. doi: 10.1016/j.egypro.2014.11.179.

[21] P. Tielens and D. van Hertem. Grid Inertia and Frequency Control in Power Systems with High Penetration of Renewables, 2012. URL `https://tinyurl.com/h24h6uf`.

[22] J. Morren, J. Pierik, and de Haan, S. W. H. Inertial response of variable speed wind turbines. *Electric Power Systems Research*, 76(11):980–987, 2006. doi: 10.1016/j.epsr.2005.12.002.

[23] Parsons Brinckerhoff. CO_2 Capture at Gas Fired Power Plants, 2012. URL `https://tinyurl.com/zanvrrr`.

[24] A. J. Seebregts. Gas-Fired Power: International Energy Agency Energy Technology Systems Analysis Programme (IEA ETSAP) - Technology (Brief (E02, 2010. URL `https://tinyurl.com/ntmefqh`.

[25] M. Nimtz and H.-J. Krautz. Flexible operation of CCS power plants to match variable renewable energies: European Geosciences Union General Assembly. *Energy Procedia*, 40:294–303, 2013. doi: 10.1016/j.egypro.2013.08.034.

[26] P. Versteeg, D. L. Oates, E. Hittinger, and E. S. Rubin. Cycling coal and natural gas-fired power plants with CCS. *Energy Procedia*, 37:2676–2683, 2013. doi: 10.1016/j.egypro.2013.06.152.

[27] N. Mac Dowell and M. Fajardy. On the potential for BECCS efficiency improvement through heat recovery from both post-combustion and oxy-combustion facilities. *Faraday discussions*, 192:241–250, 2016. ISSN 1359-6640. doi: 10.1039/C6FD00051G.

[28] M. Fajardy and N. Mac Dowell. Can BECCS deliver sustainable and resource efficient negative emissions? *Energy Environ. Sci.*, 1(1):59, 2017. ISSN 1754-5692. doi: 10.1039/c7ee00465f.

[29] M. Bui, M. Fajardy, and N. Mac Dowell. Bio-energy with CCS (BECCS) performance evaluation: Efficiency enhancement and emissions reduction. *Applied Energy*, 195:289–302, 2017. doi: 10.1016/j.apenergy.2017.03.063.

[30] S. Pfenninger and I. Staffell. Rewnewables ninja, 2016. URL `https://renewables.ninja`.

[31] C. Mone, A. Smith, B. Maples, and M. Hand. 2013 Cost of Wind Energy Review, 2015. URL https://tinyurl.com/ybgtb3a7.

[32] Parsons Brinckerhoff. Solar PV cost update: for Department of Energy and Climate Change, 2012. URL https://tinyurl.com/yamn3z47.

[33] Department of Energy & Climate Change. Review of the generation costs and deployment potential of renewable electricity technologies in the UK: Study Report, 2011. URL https://tinyurl.com/y9fgr9zp.

[34] Electricity interconnection: Sweden - Lithuania (Nordbalt), 2013. URL https://tinyurl.com/y7v2pvvo.

[35] M. Junginger, A. Faaij, and W. Turkenburg. Cost Reduction Prospects for Offshore Wind Farms. *Wind Engineering*, 28(1):97–118, 2004. ISSN 0309-524X. doi: 10.1260/0309524041210847.

[36] MWH Americas Inc. Technical Analysis of Pumped Storage and Integration with Wind Power in the Pacific Northwest. page 166, 2009. URL https://tinyurl.com/ydeqqolj.

[37] B. B. McKeon, J. Furukawa, and S. Fenstermacher. Advanced lead-acid batteries and the development of grid-scale energy storage systems. *Proceedings of the IEEE*, 102(6):951–963, 2014. ISSN 0018-9219. doi: 10.1109/JPROC.2014.2316823.

[38] S. Matteson and E. Williams. Residual learning rates in lead-acid batteries: Effects on emerging technologies. *Energy Policy*, 85:71–79, 2015. doi: 10.1016/j.enpol.2015.05.014.

[39] National Grid. Data Explorer - Real Time Demand Data: Historic, 2015. URL http://tinyurl.com/kbe65ca.

[40] I. Staffell and S. Pfenninger. Using bias-corrected reanalysis to simulate current and future wind power output. *Energy*, 114:1224–1239, 2016. doi: 10.1016/j.energy.2016.08.068.

[41] S. Pfenninger and I. Staffell. Long-term patterns of European PV output using 30 years of validated hourly reanalysis and satellite data. *Energy*, 114:1251–1265, 2016. doi: 10.1016/j.energy.2016.08.060.

[42] P. Heptonstall, R. Gross, and F. Steiner. The costs and impacts of intermittency – 2016 update, 2017. URL https://tinyurl.com/y7bwbuo4.

[43] National Grid plc. System Operability Framework 2016, 2016. URL https://tinyurl.com/guglwvy.

[44] Department of Energy & Climate Change. Updated energy and emissions projections 2015, 2015. URL http://tinyurl.com/n5a9yxv.

[45] I. Staffell. Electric Insights, 2017. URL http://electricinsights.co.uk/.

[46] European Network of Transmission System Operators for Electricity. Statistical Database, 2015. URL https://www.entsoe.eu/.

[47] Committee on Climate Change. Power sector scenarios for the fifth carbon budget, 2015. URL http://tinyurl.com/ycb58x74.

[48] Department of Business, Energy & Industrial Strategy. Digest of United Kingdom Energy Statistics 2016, 2016. URL https://tinyurl.com/yaqn5pr3.

[49] National Grid Electricity plc. Special Condition 2K.4 – Transmission Losses Report: Reporting Period 1 April 2015 to 31 March 2016, 2016. URL https://tinyurl.com/y8zo54m6.

[50] Sohn Associates Limited. Electricity Distribution Systems Losses: prepared for office of gas and electricity markets (ofgem), 2009. URL https://tinyurl.com/joarop2.

[51] A. Flamm and D. Scott. Electricity Balancing Significant Code Review - Final Policy Decision, 2014. URL https://tinyurl.com/d9nyvrn.

[52] Department of Energy & Climate Change. Fossil fuel price projections: 2015, 2015. URL https://tinyurl.com/y9wxuktv.

[53] N. Seifkar, X. Lu, M. Withers, R. Malina, R. Field, S. Barrett, and H. Herzog. Biomass to Liquid Fuels Pathways: A Techno-Economic Environmental Evaluation, 2015. URL https://tinyurl.com/yahpsbn5.

[54] World Nuclear Association. The Economics of Nuclear Power, 2017. URL https://tinyurl.com/h8lxckv.

[55] C. F. Heuberger, I. Staffell, N. Shah, and N. Mac Dowell. Electricity Systems Optimisation with capacity eXpansion and Endogenous technology Learning (ESO-XEL), 2017. URL https://zenodo.org/record/1048943.

[56] C. F. Heuberger and N. Mac Dowell. Electricity Systems Optimisation with capacity eXpansion and Endogenous technology Learning (ESO-XEL): Myopic Foresight Option., 2018. URL https://zenodo.org/record/1212298.

[57] A. Poullikkas. A comparative overview of large-scale battery systems for electricity storage. *Renewable and Sustainable Energy Reviews*, 27:778–788, 2013. doi: 10.1016/j.rser.2013.07.017.

[58] I. Staffell. Measuring the progress and impacts of decarbonising British electricity. *Energy Policy*, 102:463–475, 2017. doi: 10.1016/j.enpol.2016.12.037.

[59] S. Consonni, G. Lozza, G. Pelliccia, S. Rossini, and F. Saviano, editors. *Chemical-Looping Combustion for Combined Cycles With CO_2 Capture*, 2004. doi: 10.1115/GT2004-53503.

[60] R. Porrazzo, G. White, and R. Ocone. Techno-economic investigation of a chemical looping combustion based power plant. *Faraday discussions*, 192:437–457, 2016. ISSN 1359-6640. doi: 10.1039/C6FD00033A.

[61] M. Schnellmann, C. F. Heuberger, S. A. Scott, J. S. Dennis, and N. Mac Dowell. The Role and Value of Chemical Looping Combustion in Electricity Systems of the Future. *International Journal of Greenhouse Gas Control*, 73:1–15, 2018. URL https://doi.org/10.1016/j.ijggc.2018.03.016.

[62] M. K. Rowinski, T. J. White, and J. Zhao. Small and medium sized reactors (SMR): A review of technology. *Renewable and Sustainable Energy Reviews*, 44:643–656, 2015. doi: 10.1016/j.rser.2015.01.006. URL http://www.sciencedirect.com/science/article/pii/S1364032115000167.

[63] D. Shropshire, A. Purvins, I. Papaioannou, and I. Maschio. Benefits and cost implications from integrating small flexible nuclear reactors with off-shore wind farms in a virtual power plant. *Energy Policy*, 46:558–573, 2012. doi: 10.1016/j.enpol.2012.04.037. URL http://dx.doi.org/10.1016/j.enpol.2012.04.037.

[64] J. Vujić, R. M. Bergmann, R. Škoda, and M. Miletić. Small modular reactors: Simpler, safer, cheaper? *Energy*, 45(1):288–295, 2012. doi: 10.1016/j.energy.2012.01.078. URL http://linkinghub.elsevier.com/retrieve/pii/S036054421200093X.

[65] G. Iyer, N. Hultman, S. Fetter, and S. H. Kim. Implications of small modular reactors for climate change mitigation. *Energy Economics*, 45:144–154, 2014. doi: 10.1016/j.eneco.2014.06.023. URL http://dx.doi.org/10.1016/j.eneco.2014.06.023.

[66] Atkins. Power plant siting study: Project summary report, 2015. URL https://tinyurl.com/ybwyyj7g.

[67] C. F. Heuberger, E. S. Rubin, I. Staffell, N. Shah, and N. Mac Dowell. Power Capacity Expansion Planning Considering Endogenous Technology Cost Learning. *Applied Energy*, 204:831–845, 2017. URL https://doi.org/10.1016/j.apenergy.2017.07.075.

[68] GAMS Development Corporation. GAMS 24.7.4, 2017. URL http://www.gams.com/.

[69] IBM. IBM ILOG CPLEX Optimizer 12.3, 2017. URL https://tinyurl.com/j78vao4.

[70] B. Hua, R. Baldick, and J. Wang. Representing operational flexibility in generation expansion planning through convex relaxation of unit commitment. *IEEE Transactions on Power Systems*, 33(2):2272–2281, 2017. ISSN 08858950. doi: 10.1109/TPWRS.2017.2735026.

[71] Q. Kha Tran. *Importance Sampling for Stochastic Programming*. Ph.D., Imperial College London, London, 2016. URL https://tinyurl.com/ybtb5x9m.

[72] B. Palmintier. *Incorporating operational flexibility into electric generation planning*. Ph.D., Massachusetts Institute of Technology, 2013. URL https://tinyurl.com/y94jvh25.

[73] C. F. Heuberger, I. Staffell, N. Shah, and N. Mac Dowell. A systems approach to quantifying the value of power generation and energy storage technologies in future electricity networks. *Computers & Chemical Engineering*, 107:247–256, 2017. URL https://doi.org/10.1016/j.compchemeng.2017.05.012.

[74] P. Gabrielli, M. Gazzani, E. Martelli, and M. Mazzotti. Optimal design of multi-energy systems with seasonal storage. *Applied Energy*, 2017. doi: 10.1016/j.apenergy.2017.07.142. URL `https://doi.org/10.1016/j.apenergy.2017.07.142`.

[75] N. Levin, A. Tishler, and J. Zahavi. Time step vs. dynamic optimization of generation-capacity-expansion programs of power systems. *Operations Research*, 31(5):891–914, 1983. URL `http://www.jstor.org/stable/170893`.

[76] U.S. Energy Information Administration. Model Documentation Report: System for the Analysis of G]lobal Energy Markets ((SAGE): Volume 1, 2003.

[77] D. Martinsen, V. Krey, P. Markewitz, and S. Vögele. A Time Step Energy Process Model for Germany - Model Structure and Results. *Energy Studies Review*, 14(1):33–57, 2014. ISSN 0843-4379. doi: 10.15173/esr.v14i1.480.

[78] F. G. N. Li and N. Strachan. BLUE: Behaviour Lifestyles and Uncertainty Energy model: Online Documentation Revision 03, 2017. URL `https://tinyurl.com/y8alllnf`.

[79] F. G.N. Li. Actors behaving badly: Exploring the modelling of non-optimal behaviour in energy transitions. *Energy Strategy Reviews*, 15:57–71, 2017. ISSN 2211467X. doi: 10.1016/j.esr.2017.01.002.

[80] H. Waisman, C. Guivarch, F. Grazi, and J. C. Hourcade. The IMACLIM-R model: Infrastructures, technical inertia and the costs of low carbon futures under imperfect foresight. *Climatic Change*, 114(1):101–120, 2012. ISSN 0165-0009. doi: 10.1007/s10584-011-0387-z.

[81] I. Keppo and M. Strubegger. Short term decisions for long term problems – The effect of foresight on model based energy systems analysis. *Energy*, 35(5):2033–2042, 2010. doi: 10.1016/j.energy.2010.01.019.

[82] S. Babrowski, T. Heffels, P. Jochem, and W. Fichtner. Reducing computing time of energy system models by a myopic approach. *Energy Systems*, 5(1):65–83, 2014. ISSN 1868-3967. doi: 10.1007/s12667-013-0085-1.

[83] F. Fuso Nerini, I. Keppo, and N. Strachan. Myopic decision making in energy system decarbonisation pathways. a uk case study. *Energy Strategy Reviews*, 17:19–26, 2017. ISSN 2211467X. doi: 10.1016/j.esr.2017.06.001.

[84] S. Pye, F. G. N. Li, J. Price, and B. Fais. Achieving net-zero emissions through the reframing of uk national targets in the post-paris agreement era. *Nature Energy*, 2(3):17024, 2017. ISSN 2058-7546. doi: 10.1038/nenergy.2017.24.

[85] Committee on Climagte Change. UK climate action following the Paris Agreement, 2016. URL `https://tinyurl.com/ot5sc9g`.

[86] Staffell, I., Boßmann, T. The shape of future electricity demand: Exploring load curves in 2050s Germany and Britain. *Energy*, 90(2):1317–1333, 2015. URL `doi:10.1016/j.energy.2015.06.082`.

[87] Department of Business, Energy & Industrial Strategy. Electricity: Chapter 5, Digest of United Kingdom Energy Statistics (DUKES), 2017. URL `https://tinyurl.com/nw9pnk5`.